ELSEVIER

Journal of Power Sources 108 (2002) 163–173

JOURNAL OF POWER SOURCES

www.elsevier.com/locate/jpowsour

Surface film formation on nickel electrodes in a propylene carbonate solution at elevated temperatures

Ryo Mogi[a,b], Minoru Inaba[a,*], Yasutoshi Iriyama[a], Takeshi Abe[a], Zempachi Ogumi[a]

[a]*Department of Energy and Hydrocarbon Chemistry, Graduate School of Engineering, Kyoto University, Sakyo-ku, Kyoto 606-8501, Japan*
[b]*Shibukawa Laboratory, Kanto Denka Kogyo Co. Ltd., 1497 Shibukawa, Gunma 377-8513, Japan*

Received 6 December 2001; accepted 22 December 2001

Abstract

The effect of temperature on surface film formation on nickel electrode was studied in 1 mol dm^{-3} bis(perfluoroethylsulfonyl)imide dissolved in propylene carbonate by atomic force microscopy (AFM) and ac impedance spectroscopy. Cyclic voltammetry measurements revealed that electrolyte decomposition reactions are accelerated at elevated temperatures, especially at 60 and 80 °C. In situ AFM measurements showed that the film formation is fast and the resulting surface film is thicker at 80 °C than at room temperature. Furthermore, it was confirmed by ac impedance measurements that the resistance of surface film was very low at elevated temperatures. These results were discussed in relation to superior cycling characteristics of lithium deposition and dissolution at the elevated temperatures.

Keywords: Nickel electrode; Electrolyte decomposition; Surface film; Elevated temperature; In situ atomic force microscopy

1. Introduction

Lithium metal is the most attractive material as a negative electrode in rechargeable batteries [1]. However, dendritic deposition of lithium, which lowers the cycling efficiency and causes safety issues, has prevented lithium metal from wide use in commercial available rechargeable batteries [1–3]. It is generally known that protective surface film, which is often called solid electrolyte interface (SEI), is formed on metallic lithium electrode and its physical and chemical properties greatly affect the morphology of deposited lithium [4,5]. In order to suppress the dendritic deposition, many researchers have extensively studied the correlation between the physicochemical properties of surface film and the morphology of deposited lithium using a variety of analytical tools. These include ac impedance spectroscopy [5–12], scanning vibrating electrode microscopy [13,14], surface potential microscopy (SPoM) [15], X-ray photoelectron spectroscopy (XPS) [10–12,16–19], Fourier transform infrared spectroscopy (FT-IR) [17–20], electrochemical quartz crystal microbalance (EQCM) [21–25], atomic force microscopy (AFM) [26–29], and temperature programmed decomposition–gas chromatography–mass spectroscopy (TPD–GC–MS) [20]. These studies have revealed that surface film on lithium consists of reductively decomposed products of solvent molecules, lithium salts and contaminants such as H_2O, CO_2, and O_2.

We have previously reported that the efficiency and cycle life for lithium deposition and dissolution are improved at elevated temperatures of 60 and 80 °C in 1 M LiBETI/PC [30,31]. In situ AFM observation revealed that a densely packed layer of particle-like precipitates is uniformly formed on lithium metal at the elevated temperatures. The surface morphology did not change at all during further deposition and dissolution processes, which meant that the layer effectively worked as a protective surface film and underneath it, a uniform layer of lithium was deposited. The rate for electrolyte decomposition is enhanced at elevated temperatures, which results in a rapid formation of the surface layer and improves self-reparability when being damaged. We, therefore, concluded that the dense and uniform structure of the surface film, its fast self-reparability and possibly enhanced surface diffusion of deposited lithium atoms, suppressed dendritic deposition of lithium and improved the cycling characteristics at the elevated temperatures. However, the detailed mechanism for film formation at the elevated temperatures has not been clarified yet. This is partly because the potential of metallic lithium electrode cannot be controlled and thus surface film formation is very fast. Decomposition processes of non-aqueous solutions containing lithium salts have been extensively

* Corresponding author. Tel.: +81-5-53-598; fax: +81-5-53-889.
E-mail address: inaba@scl.kyoto-u.ac.jp (M. Inaba).

0378-7753/02/$ – see front matter
PII: S0378-7753(02)00031-9

studied not only on lithium metal, but also on other non-active metallic electrodes such as Au [21–24,26,32–36], Ni [25,34,37–39], Ag [32–35,39], Cu [27–29,35,39,40], Pt [32], Ti [39] at potentials higher than lithium deposition. Because the rates for the decomposition processes can be controlled by changing the potentials, these non-active metallic electrodes are very useful to study the decomposition processes of electrolyte solution and the resulting surface film formation. In the present study, we used nickel plate as a model metallic electrode and investigated surface film formation processes on the nickel metal at elevated temperatures by in situ AFM and ac impedance spectroscopy.

2. Experimental

The electrolyte solution used in the present study was a 1 mol dm^{-3} (M) solution of lithium bis(perfluoroethylsulfonyl)imide ($LiN(C_2F_5SO_2)_2$, LiBETI, 3 M) dissolved in propylene carbonate (PC, Kishida Reagents Chemicals). The water content of the solution was less than 30 ppm, which was measured with a Karl-Fischer moisture titrator. The working electrode was nickel plate polished to a mirror finish and the counter, and reference electrodes were lithium foil.

In situ AFM images were obtained with a PicoSPM® system (molecular imaging) equipped with a PicoStat® potentiostat (molecular imaging). A laboratory-made polytetrafluoroethylene (PTFE) cell was set on a heating sample stage and used for in situ electrochemical AFM measurements. The surface area of the working electrode was fixed at 1.2 cm^2 using an O-ring. The temperature of the cell was controlled with a temperature controller (Model 330, Lake Shore). Cyclic voltammetry (CV) was performed at 5 mV s^{-1} at room temperature (RT), 40, 60, and 80 °C. AFM observation was carried out at 2.5 V versus Li^+/Li after each cycle. The temperature of the cell was cooled down to 33 °C prior to AFM observation to avoid the lens for laser beam from being fogged up. AFM images were obtained in the contact mode with a microcantilever made of silicon nitride (spring constant, 0.68 N m^{-1}). During each potential cycle, the cantilever was moved out of the solution because current distributiion beneath the tip would have been disturbed by its presence. AFM observation was also performed holding the potential of the nickel electrode at constant potentials. In these measurements, the cell was kept at an elevated temperature for 15 min and then cooled down to 33 °C for AFM observation. All AFM measurements were carried out in an argon-filled glove box (Miwa, MDB-1B + MM3-P60S) with a dew point lower than −60 °C.

A sealed cell made of PTFE was used for ac impedance measurements. The surface area of the working electrode was 0.8 cm^2. The cell was assembled in an argon-filled glove box and impedance measurements were performed in an electric oven kept at elevated temperatures. The nickel electrode was polarized at a constant potential for a sufficient time until the current became negligible (typically < 1 μA). The impedance was measured with a frequency analyzer (SI 1255, Solartron) and a potentiostat (Model 273A, EG&G PAR) over the frequency range of 1–10 kHz. The alternating amplitude was 5 mV, unless otherwise noted. The potential was successively lowered by 0.5 V from 3.0 V, except that the final potential was set at 0.05 V instead of 0.0 V to avoid lithium deposition.

3. Results and discussion

3.1. Cyclic voltammetry

Fig. 1 shows cyclic voltammograms obtained on nickel electrode in 1 M LiBETI/PC at RT, 40, 60, and 80 °C. Three major cathodic peaks were observed at 0.9, 0.5, and 0.2 V in the first cycle at RT. The peak currents increased with temperature and were almost doubled at 40 °C. The peak at 0.9 V at RT was shifted to 1.1 V at 40 °C, while the potentials of the other two peaks remained almost unchanged. At 60 °C, the peak currents further increased. A broad shoulder appeared at 0.7 V, and the peak at 0.5 V became sharp. It is clear that these peaks overlapped at around 0.5 V at 40 °C and lower. The voltammogram at the first cycle obtained at 80 °C was very similar to that at 60 °C, except that the peak at 0.7 V was not a shoulder but an obvious separate peak.

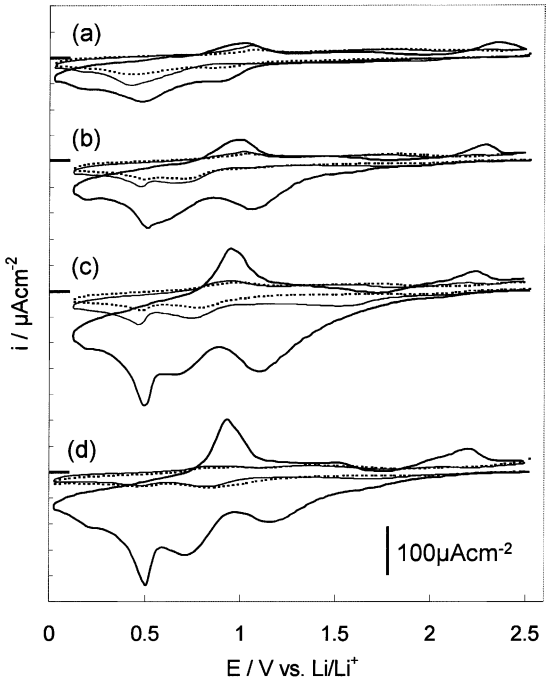

Fig. 1. Cyclic voltammograms on Ni electrode in 1 M LiBETI/PC at (a) RT, (b) 40 °C, (c) 60 °C, (d) 80 °C. The sweep rate was 5 mV s^{-1}. Bold solid, solid and dashed lines shows CVs in the first, second and fifth cycles, respectively.

Many researchers have studied electrochemical reactions on metallic electrodes, such as Ni, Au, Cu, Ag, Pt, Ti in non-aqueous electrolyte solutions of lithium salts [21–29,32,40]. Most of them reported that dissolved oxygen is reduced at around 2.0 V, and reduction of H_2O occurs in the range 1.0–1.5 V. Aurbach et al. [33] proposed that O_2 is reduced to O_2^- to form mainly LiO_2, whereas H_2O is reduced to LiOH. In PC-based solutions, reductive decomposition of PC occurs at potentials below 1.5 V on Au electrode [33]. Several groups estimated the molecular weights of decomposed products that precipitated on metallic electrodes in PC-based solutions using EQCM [21–25]. Aurbach et al. [26,33,34] have suggested that PC decomposes to form lithium alkyl carbonates (RCO_3Li), and confirmed the presence of these compounds by FT-IR. The couple of the cathodic peak at 0.5 V and the anodic peak at 1.0 V have been generally assigned to underpotential deposition and stripping (UPD and UPS), respectively, of lithium on Au [21–24,33,35], Ni [37,39], Cu [39], Ag [39], and Ti [39]. Some evidences for lithium UPD have been provided by EQCM [21–24]. However, Fujieda et al. [40] reported that a peak was seen at 0.5 V on Cu electrode even when a Li^+-free electrolyte solution was used and they assigned the peak to decomposition of contaminants.

At RT in Fig. 1(a), noticeable cathodic peaks corresponding to the reduction of O_2 and H_2O above 1.0 V were not observed, which confirmed that contamination of the electrolyte solution with O_2 and H_2O was negligible in the present study. It is not easy to specify each peak below 1.0 V; however, all the cathodic peaks are attributable to reductive decomposition of the electrolyte solution except that the peak at 0.5 V may be assigned to lithium UPD. These cathodic peaks were enhanced and some of them shifted to more positive potentials at elevated temperatures, which shows that the electrolyte decomposition reactions were accelerated by a rise of temperature. It is, therefore, reasonable to think that thicker surface film was formed on Ni electrode in the first cycle at elevated temperatures.

The peak currents decreased in subsequent cycles at each temperature. This was caused by the formation of protective surface film during the first cycle. The peak currents gradually decreased every cycle up to the fifth cycle at RT, whereas the decrease after the first cycle was more dramatic at elevated temperatures. In particular, the voltammogram of the fifth cycle was almost superimposable on that of the second cycle at 80 °C, which indicated that the surface film was formed rapidly and had superior stability and passivating ability.

3.2. In situ AFM observations

Images (a) to (d) in Fig. 2, show AFM images of the surface morphologies of Ni observed after the five cycles of CV at RT, 40, 60, and 80 °C, respectively in Fig. 1. There was no deposit at each temperature before CV and many grooves made from polishing were observed on nickel substrate (see, e.g. Fig. 3(a)). The grooves became indistinct after five cycles of CV, but they were still visible at RT and 40 °C. This indicates that surface film formation was not enough to cover the whole surface of the electrode at the lower temperatures and hence the electrode was less passivated as shown in Fig. 1. Particle-like deposits of 50–150 nm in diameter appeared sparsely after the fifth cycle although they were not observed after the first cycle at RT (not shown). The particle became larger in their size and increased in their number with a rise of temperature. Particles of about 200 nm in diameter were observed at 60 and 80 °C, and the grooves on the substrates were no longer visible. At 80 °C, many particles were observed even after the first cycle (not shown) and the whole surface was covered with a layer of particle-like deposits after the fifth cycle. We observed several different areas and confirmed that there was a uniform covering of the deposits on the surface. These results of AFM observation are consistent with those obtained from the CV measurements in the preceding section, i.e. electrolyte decomposition is accelerated at elevated temperatures and the resulting surface film passivated the nickel electrode strongly at 80 °C.

In order to correlate the morphological changes of the electrode surface with the cathodic peaks of CV in Fig. 1, we observed the surface at constant potentials. The surface morphologies obtained at open circuit voltage (OCV) (∼3 V), 1.5, 1.3, 0.6, 0.5, and 0.1 V at RT are shown in Fig. 3. At 1.5 V (Fig. 3(b)), the image of the surface became unclear because many noisy lines ran across the image. These noisy lines are evidence for scratching of the surface with the microcantilever under the contact mode operation. Because these lines were not observed at OCV in Fig. 3(a), this is the first change of surface morphology. As mentioned earlier, the cathodic peak at around 1.5 V is generally assigned to the reduction of H_2O, whereas Aurbach et al. [33,34] assigned it to the decomposition of electrolyte solution by in situ FT-IR analysis. They further confirmed the formation of surface film at 1.5 V on Au in 0.5 M $LiPF_6$ dissolved in a 1:1 mixture of ethylene carbonate (EC) and dimethyl carbonate (DMC) by in situ AFM [26]. In Fig. 2(a) in the present study, only minor current was observed at around 1.5 V. This current is attributable to the reduction of H_2O and/or the electrolyte solution and the observed surface morphological change at 1.5 V indicates the earliest step of surface film formation on Ni electrode. The film formed at 1.5 V did not seem to be complete and it may be so thin and soft that it is easily scraped off during probe scanning.

The noisy lines disappeared at 1.3 V and lower as shown in Fig. 3(c) and this indicates that the surface film changed to be more solid. Although the grooves on the nickel electrode were seen at 1.5 V, they became indistinct with lowering the potential. When the potential was lowered further, almost no change was observed down to 0.6 V (Fig. 3(d)). Remarkable morphological changes that can be directly correlated with the cathodic peak at 0.9 V in Fig. 1(a) were not observed in the range 1.3–0.6 V. This fact indicates that the peak gave

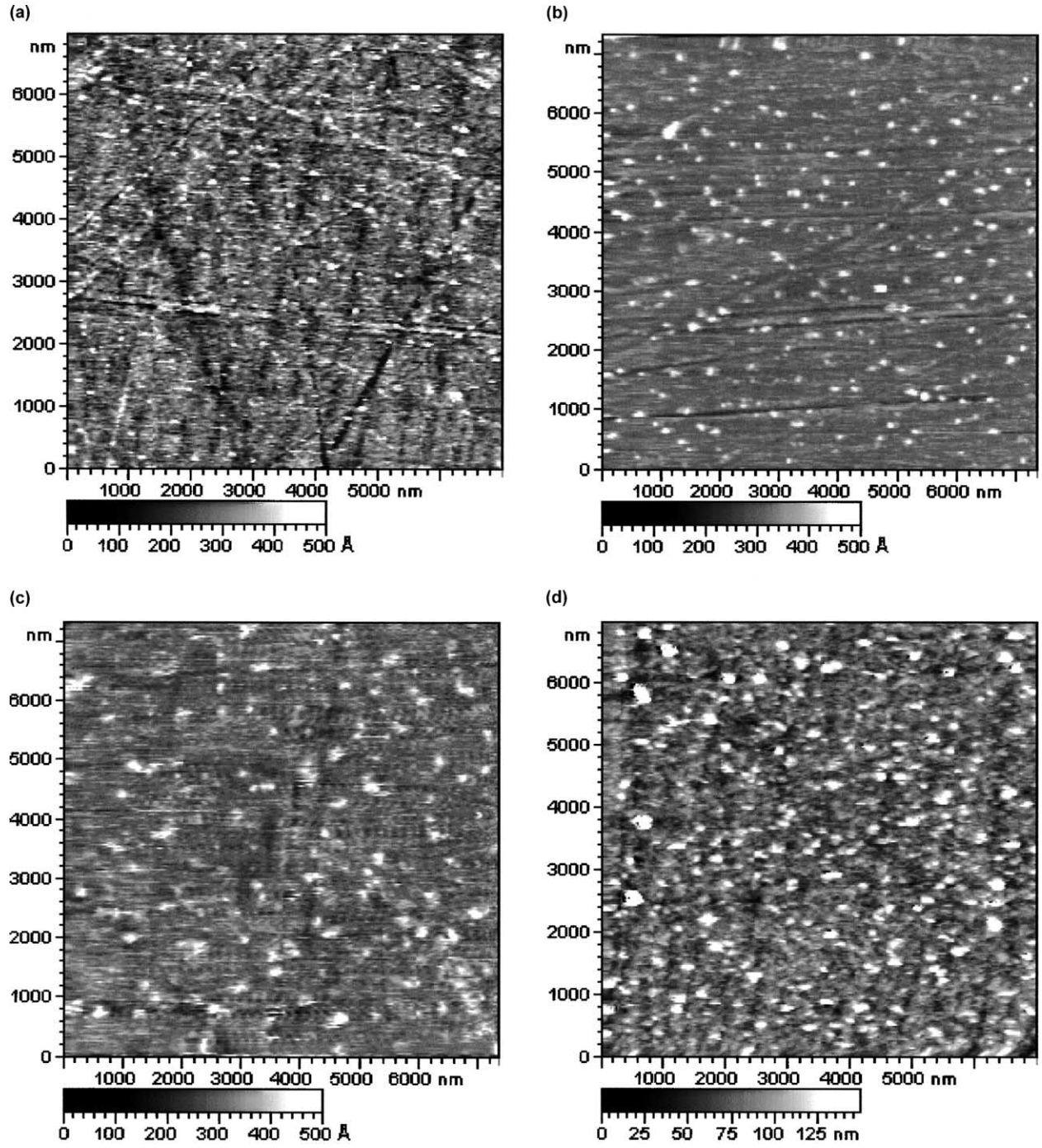

Fig. 2. AFM images (7 μm × 7 μm) of the surface morphology on nickel substrate obtained after five cycles of CV in 1 M LiBETI/PC at (a) RT, (b) 40 °C, (c) 60 °C, (d) 80 °C.

only soluble reduction products. At 0.5 V (Fig. 3(e)), particle-like deposits of 100–200 nm in diameter appeared on the surface. This morphological change obviously can be correlated with the cathodic peak at 0.5 V, and it is clear that the reactions occurred at 0.5 V were different from those above 0.6 V. The particle size increased with lowering the potential and became 200–300 nm in diameter at 0.1 V as shown in Fig. 3(f). Morigaki et al. [29] observed surface morphological changes of Cu electrode in 1 M $LiPF_6$/EC + DMC and /EC + diethyl carbonate (DEC) by in situ AFM. They also observed particle-like deposits of 300 (EC + DMC) and 300–600 nm (EC + DEC) in diameter at potentials between 1.0 and 0.05 V.

AFM observation was carried out at 80 °C in a similar manner and the results are shown in Fig. 4. The grooves made from polishing became barely visible even at 1.5 V (Fig. 4(a)), which shows that the amount of deposits was much larger at 80 °C. Noisy lines caused by surface scratching were not

seen at 1.5 V; hence, the surface film formed at 80 °C seemed to be more solid than that formed at RT. The cathodic current at around 1.5 V was about five times larger at 80 °C than that at RT as shown by the voltammograms in Fig. 1. It is thus clear that reductive decomposition of the electrolyte solution occurred very rapidly at 80 °C. In addition, the deposition occurred favorably along the grooves that were made from polishing. At 1.1 V in Fig. 4(b), the surface became rough and particle-like deposits appeared. This change corresponds to the peak at 1.2 V in CV. The image is very noisy, which shows that the tip trailed protrusive part of the deposits. This scratching effects are shown in more detail in Fig. 4(c)–(e). First, a 3 μm × 3 μm area was observed several times at 0.7 V (Fig. 4(c)), and then an expanded area of 7 μm × 7 μm including the 3 μm × 3 μm area was observed. Fig. 4(d) shows the image obtained in the first scan of the 7 μm × 7 μm area, in which a dark square, caused by scratching with the microcantilever during the

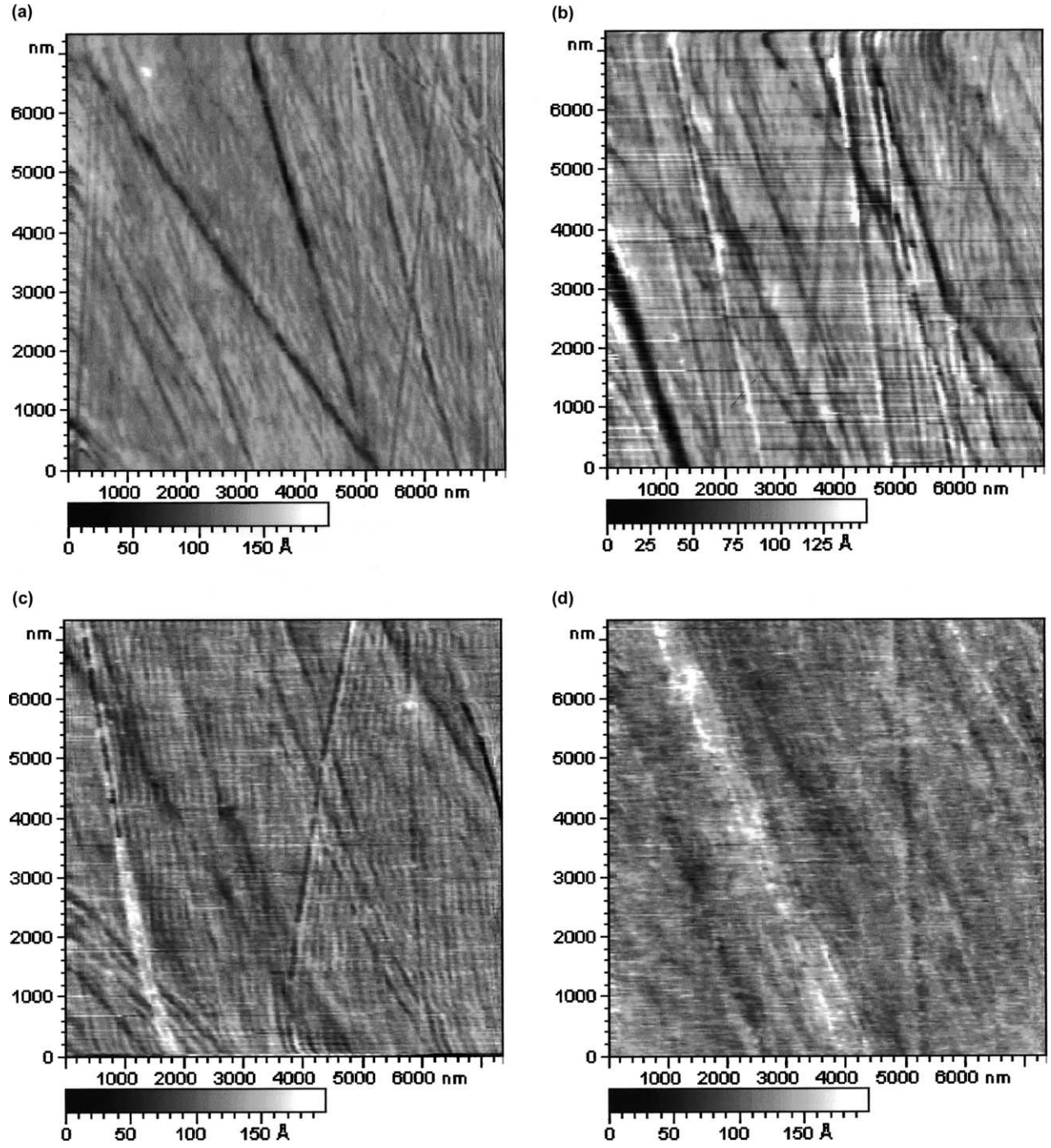

Fig. 3. AFM images (7 μm × 7 μm) of the surface morphology on nickel substrate in 1 M LiBETI/PC at RT. Observations were carried out at (a) OCV, (b) 1.5 V, (c) 1.3 V, (d) 0.6 V, (e) 0.5 V, (f) 0.1 V.

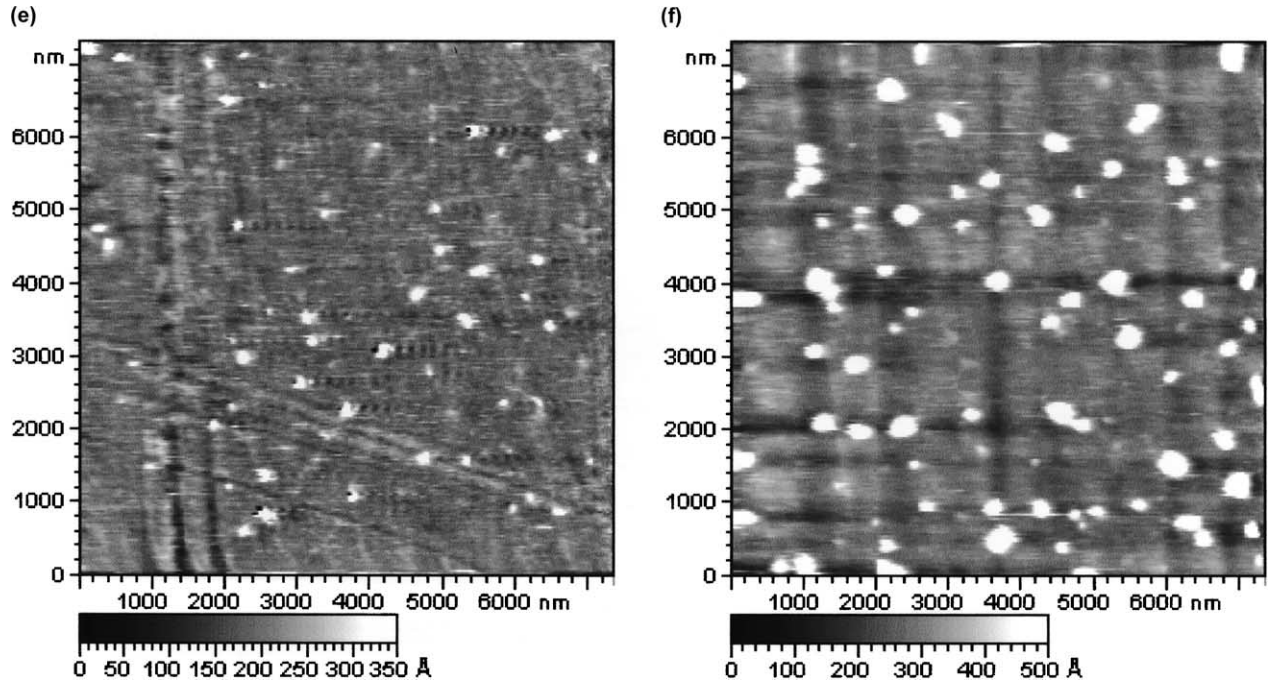

Fig. 3. (*Continued*).

initial scanning in the 3 μm × 3 μm area, is seen at the center of the image. The image obtained in the second scan is shown Fig. 4(e). The square at the center became indistinct, which means that the outer area was also scratched in the first scan. However, we were not able to scrape off the surface film completely and to reach the nickel surface during the following several scans. It is, therefore, considered that the inmost thin layer was strongly adhered to the nickel surface.

Almost no change was observed in the potential range 1.1–0.6 V, as shown in Fig. 4(b)–(f). This fact suggests again that part of the products formed in this potential range are soluble in the electrolyte solution. The morphology changed at 0.5 V as shown in Fig. 4(g), in which many particles larger than 200 nm appeared. The appearance of large particles can be correlated with the sharp cathodic peak at 0.5 V. It should be noted that this peak did not shift even at 80 °C, indicating that the reaction taking place at 0.5 V was fast and clearly different from the reactions at more positive potentials. The particle size grew up with lowering the potential down to 0.1 V as shown in Fig. 4(h). Because the cantilever dragged the large particles upon scanning, the shapes of the particles in these images do not exhibit their actual shapes. The real particle size may have been smaller. The images in Figs. 3 and 4 obtained at constant potentials were somewhat different from those obtained after five cycles of CV in Fig. 2. For example, the sizes of the particles formed at a constant potential of 0.5 V were larger than those formed by CV. This may be due to the difference in the experimental conditions; e.g. the rate for nucleation and growth of nuclei must be different between the two methods, which will greatly affect the particle size.

3.3. The Ac impedance measurements

Ac impedance spectra of the nickel electrode were measured at different potentials to clarify the electrochemical properties of the surface film. Fig. 5 shows the variation of the impedance spectra with potential at RT. At 3.0 V, only a line perpendicular to the Z'-axis appeared, which is typical of a blocking electrode. This impedance behavior shows that no reactions occurred at this potential. Such blocking behavior was observed down to 2.0 V. The spectrum changed slightly at 1.5 V. It was not a straight line, but had a curvature in the high frequency region. This change corresponds to the observed small current in Fig. 1(a), which was assigned to reductive decomposition of H_2O and/or electrolyte in previous sections. At 0.5 V, a depressed arc appeared in the high frequency region, being coupled with a perpendicular line in the low frequency region. At this potential, the largest cathodic peak was observed in the first cycle of CV at RT, and the particle-like deposits appeared on the surface. This arc is, therefore, attributable to the impedance of lithium ion migration through the layer of the deposits. Aurbach et al. have reported very similar impedance spectra of Ni [34,38], Au [26,34] and Ag [34] electrodes in some carbonate-based electrolyte solutions containing Li salts and assigned the arc in the high frequency region to the impedance of the surface film.

As mentioned earlier, the peak at 0.5 V may be due to the UPD of lithium. When UPD takes place, it usually gives an impedance spectrum similar to that at 0.5 V in Fig. 5, i.e. a depressed arc in the high frequency region and a linear line in the low frequency region [41,42]. Fig. 6 shows the variation of the impedance spectra with perturbation amplitude

obtained at 0.5 V. The impedance response did not change with an increase in ac amplitude in the range 5–40 mV and hence can be attributed to a process with an ohmic resistance. Consequently, the arc cannot be assigned to the charge-transfer reaction of UPD, although this does not deny the possibility that UPD occurs at 0.5 V.

The variation of the film impedance with the concentration of LiBETI was next examined at 0.5 V. After surface film was formed at 0.5 V in 1 M LiBETI/PC, the impedance was measured. The solution was successively diluted to lower concentrations by adding pure PC, and the impedance responses were obtained. The results are shown in Fig. 7, in which the resistance of the electrolyte was subtracted for clarity. The resistance of the surface film gradually increased with lowering the concentration of LiBETI. As shown in Fig. 7, ca. 20-fold dilution resulted in only a two-fold

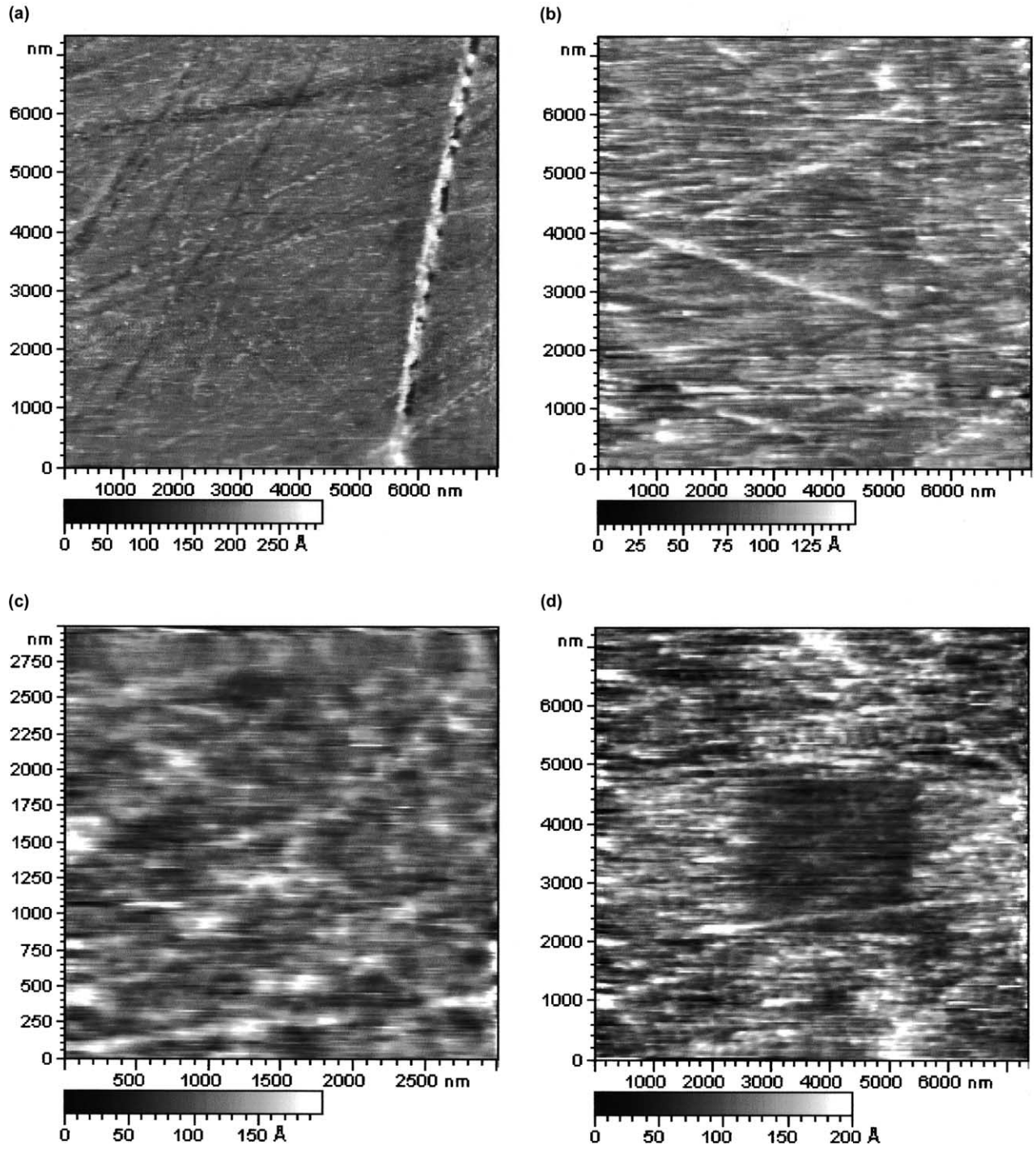

Fig. 4. AFM images of the surface morphology on nickel substrate in 1 M LiBETI/PC at 80 °C. Observations were carried out at (a) 1.5 V, (b) 1.1 V, (c–e) 0.7 V, (f) 0.6 V, (g) 0.5 V, (h) 0.1 V. (a, b, d–h) 7 μm × 7 μm; (c) 3 μm × 3 μm.

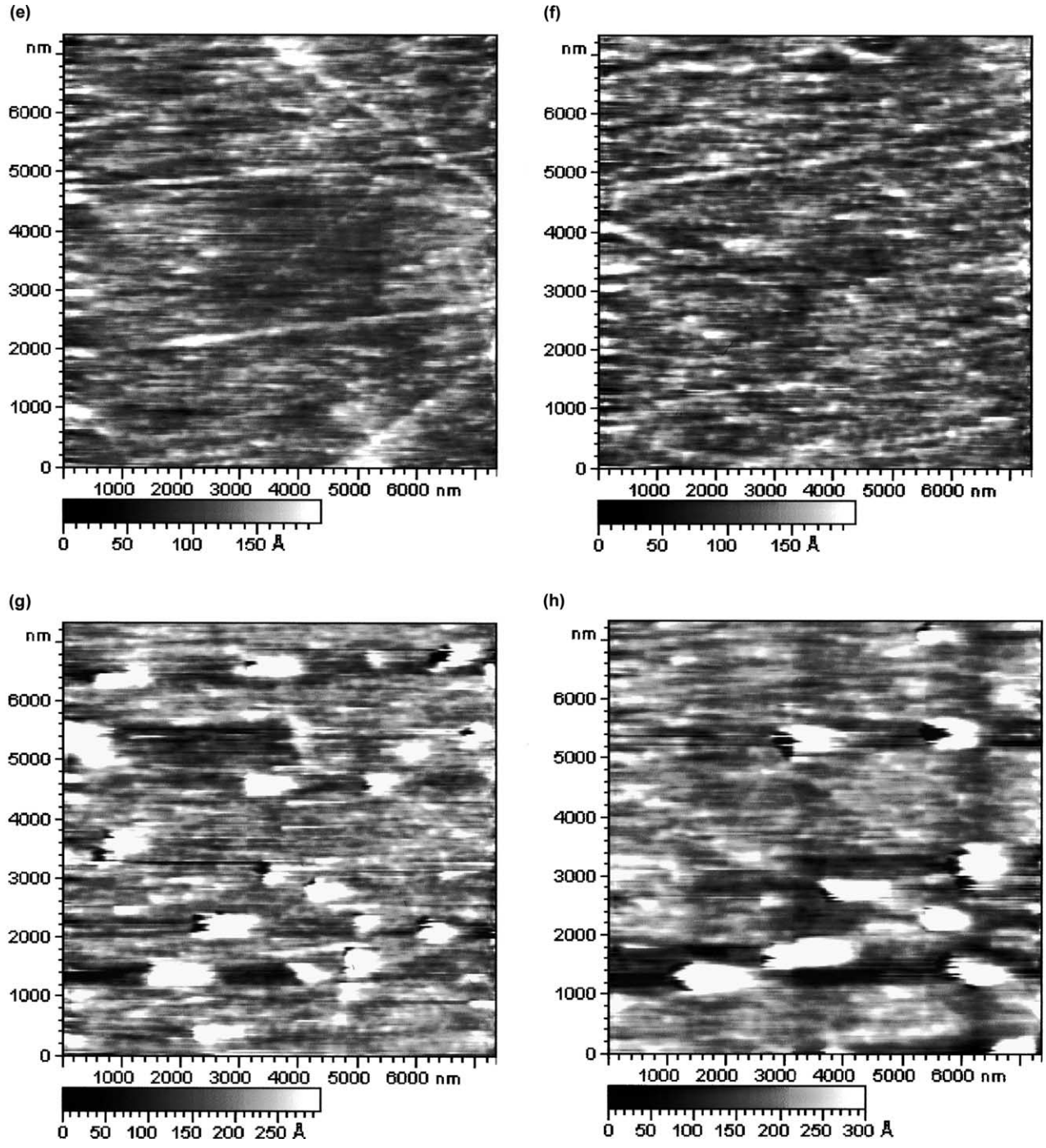

Fig. 4. (*Continued*).

increase in resistance. This is another evidence that the arc is not assigned to UPD that is a charge-transfer reaction. Because the concentration of LiBETI affected the resistance of the surface film, the lithium salt was incorporated within the surface film and participated in ion conduction in the surface film.

Fig. 8(a) shows impedance spectra at 80 °C obtained in a similar manner to Fig. 5. The resistance of the solution was 130 Ω, which was lower than the value of 330 Ω at RT. At all potentials tested, the spectra showed the behavior of a blocking electrode and no arc was seen even at 0.05 V. This means that the impedance of the surface film was negligibly low. After the measurements, the cell was cooled down to 25 °C while the potential was kept at OCV. The impedance spectrum measured at 25 °C is shown in Fig. 8(b). The resistance of the solution increased to 330 Ω and a distinct arc appeared in the high frequency region. The resistance of this arc (307 Ω) was higher than that obtained at RT (47 Ω),

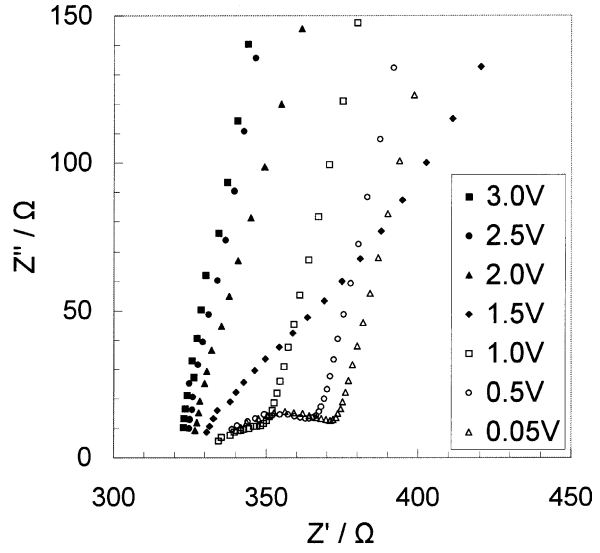

Fig. 5. Impedance spectra at Ni electrode obtained at various potentials in 1 M LiBETI/PC at RT.

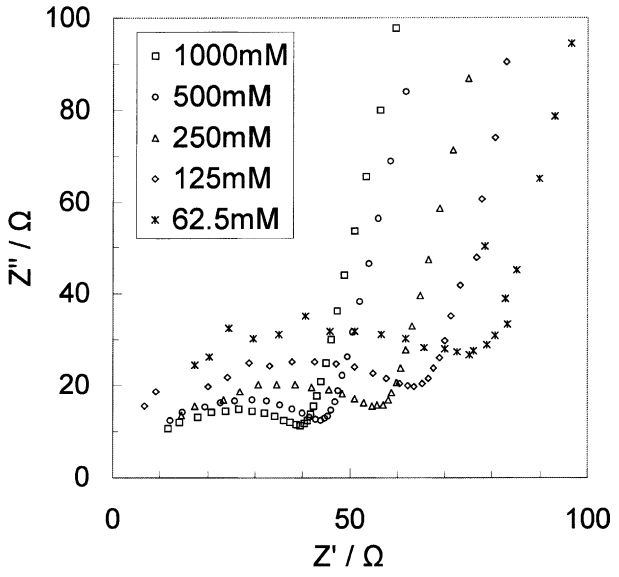

Fig. 7. Variation of the impedance of the surface film formed at 0.5 V with the concentration of LiBETI in 1 M LiBETI/PC at RT.

indicating that the surface film formed at 80 °C was thicker. This conclusion is in agreement with the results of CV and AFM measurements in the preceding sections. It should be noted that the resistance of the surface film was much lower at 80 °C than that formed at RT although surface film formation was faster and the resulting film was thicker. A high resistance of surface film tends to cause non-uniform current distribution, which accelerates the formation of dendritic lithium. Consequently, it is concluded that the low resistance of the surface film formed at 80 °C is one of the important properties to suppress the formation of dendritic lithium.

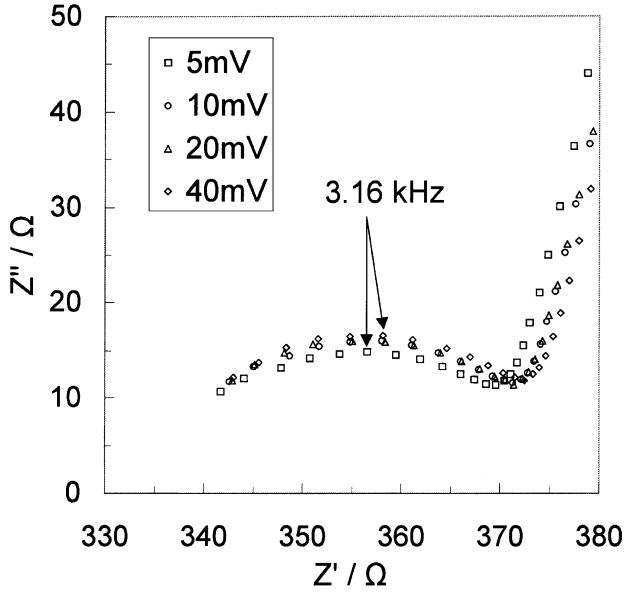

Fig. 6. Variation of the impedance of the surface film formed at 0.5 V with ac amplitude in 1 M LiBETI/PC at RT.

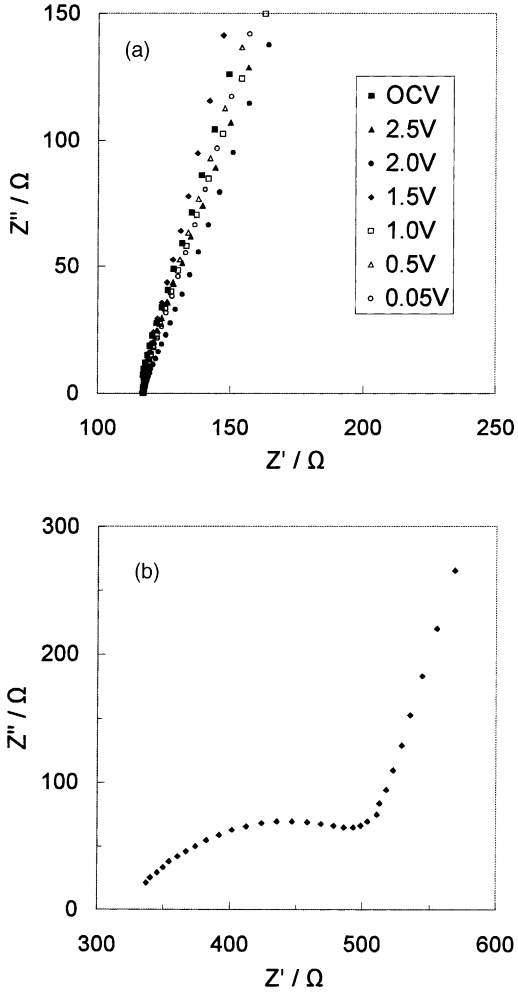

Fig. 8. (a) Impedance spectra at Ni electrode obtained various potentials in 1 M LiBETI/PC at 80 °C, (b) impedance spectrum obtained after cooled down to 25 °C.

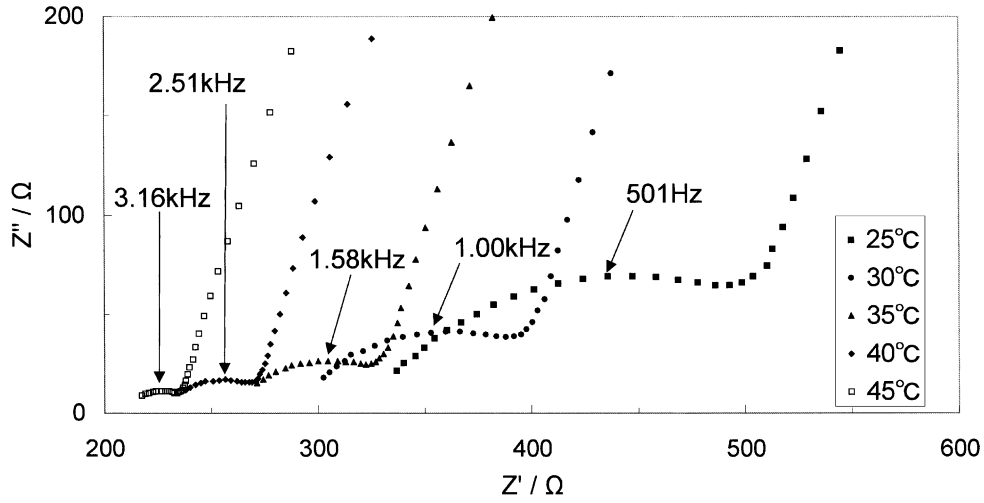

Fig. 9. Temperature dependence of the impedance spectra of the surface film formed at 0.5 V on Ni at 80 °C in 1 M LiBETI/PC.

Temperature dependence of the impedance is shown in Fig. 9. The cell was heated at 80 °C for 2 h and the impedance measurements were performed at different temperatures holding the electrode potential at 0.5 V. At 80 and 60 °C, the spectra exhibited no distinct arc because the impedance of the surface film was negligibly low. At temperatures of 45 °C and lower, the arc appeared. The resistance of the surface film increased with a drop in temperature. Fig. 10 shows the Arrhenius plot of the conductance of the surface film. The plot gave a linear line, with an activation energy (E_a) for lithium ion conduction, calculated from the slope was found to be 85.3 kJ mol^{-1}. The E_a values for lithium–electrolyte interfaces reported in the literature are rather scattered and greatly depend on the concentration and the kind of electrolyte salts, e.g. 58.8 kJ mol^{-1} in 0.5 M $LiClO_4$/PC [43], 49.8 [44], 57 [45] and 50–80 [46] kJ mol^{-1} in 1 M $LiClO_4$/PC etc. and 21.4–38.1 kJ mol^{-1} in $LiAlCl_4$/PC [47]. The value obtained in the present study seems to be somewhat higher than these reported values. It should be noted that most of the above E_a values were estimated from temperature dependence of exchange current density, i_0, at lithium metal or nickel microdisk electrodes that were covered with surface films. Therefore, some of the E_a values are not free from charge-transfer resistance, whereas others ignore the presence of the surface film as pointed out by Munichandraiah et al. [48]. In addition, most of the studies have ignored film growth at elevated temperatures during measurements. In the present work, there is no doubt that the E_a value correctly represents the activation energy for lithium ion conductance in the surface film formed at 80 °C.

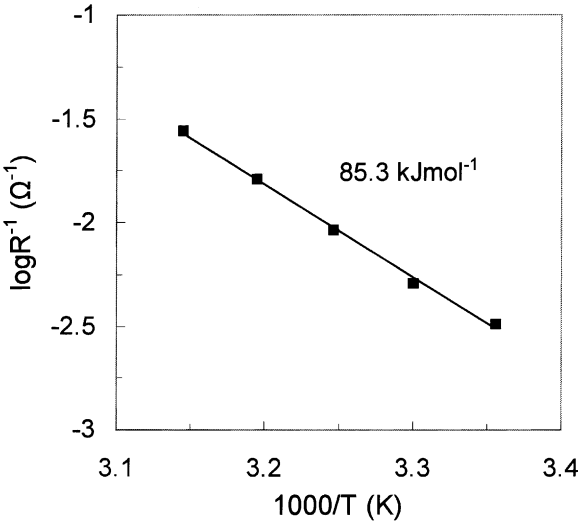

Fig. 10. Arrhenius plot of the conductance of the surface film formed at 0.5 V on Ni at 80 °C in 1 M LiBETI/PC.

4. Conclusion

The effect of temperature on surface film formation on nickel electrode was studied by AFM and ac impedance spectroscopy to clarify the mechanism that gives the improved cycling characteristics of lithium negative electrode at elevated temperatures. CV measurements revealed that electrolyte decomposition reactions are accelerated at elevated temperatures, especially at 60 and 80 °C. In situ AFM measurements showed that the film formation is fast and the resulting surface film is thicker at 80 °C. Furthermore, it was confirmed by ac impedance measurements that the resistance of surface film is very low at elevated temperatures. These results revealed the properties requisite for suppressing dendritic lithium deposition as follows: (1) surface film should be dense and uniform, (2) the film formation should be fast so that the surface is rapidly passivated and the resulting surface film is easily self-reparable when being damaged during deposition and dissolution cycles and (3) the film resistance should be as low as possible to avoid the concentration of the current. These

properties are satisfied at elevated temperatures and thus the cycling characteristics of metallic lithium electrode were greatly improved as we reported previously.

References

[1] J. Yamaki, S. Tobishima, in: J.O. Besenhard (Ed.), Handbook of Battery Materials (Part III), Wiley, Weinheim, 1999.
[2] M. Arakawa, S. Tobishima, Y. Nemoto, M. Ichimura, J. Power Sources 43/44 (1993) 27.
[3] J. Yamaki, S. Tobishima, K. Hayashi, K. Saito, Y. Nemoto, M. Arakawa, J. Power Sources 74 (1998) 219.
[4] E. Peled, J. Electrochem. Soc. 126 (1979) 2047.
[5] J.G. Thevenin, R.H. Muller, J. Electrochem. Soc. 134 (1987) 273.
[6] D. Aurbach, A. Zaban, J. Electroanal. Chem. 48 (1993) 155.
[7] N. Takami, T. Ohsaki, K. Inada, J. Electrochem. Soc. 139 (1992) 184.
[8] C. Wang, H. Nakamura, H. Noguchi, M. Yoshio, Denki Kagaku 65 (1997) 941.
[9] T. Osaka, T. Momma, T. Tajima, Y. Matsumoto, J. Electrochem. Soc. 142 (1995) 1057.
[10] K. Naoi, M. Mori, Y. Naruoka, W.M. Lamanna, R. Atanasoski, J. Electrochem. Soc. 146 (1999) 462.
[11] M. Ishikawa, S. Machino, M. Morita, J. Electroanal. Chem. 473 (1999) 279.
[12] K. Kanamura, S. Shiraishi, Z. Takehara, J. Electrochem. Soc. 143 (1996) 2187.
[13] M. Ishikawa, S. Yoshitake, M. Morita, Y. Matsuda, J. Electrochem. Soc. 141 (1994) L159.
[14] M. Ishikawa, M. Morita, Y. Matsuda, J. Power Sources 68 (1997) 501.
[15] S. Shiraishi, K. Kanamura, Z. Takehara, J. Phys. Chem. B 105 (2001) 123.
[16] N.P.W. Langenhuizen, J. Electrochem. Soc. 145 (1998) 3094.
[17] D. Aurbach, M.L. Daroux, P.W. Faguy, E. Yeager, J. Electrochem. Soc. 134 (1987) 1611.
[18] K. Morigaki, A. Ohta, J. Power Sources 76 (1998) 159.
[19] T. Osaka, T. Momma, Y. Matsumoto, Y. Uchida, J. Electrochem. Soc. 144 (1997) 1709.
[20] A. Kominato, E. Yasukawa, N. Sato, T. Ijuuin, H. Asahina, S. Mori, J. Power Sources 68 (1997) 471.
[21] D. Aurbach, A. Zaban, J. Electroanal. Chem. 393 (1995) 43.
[22] M. Moshkovich, Y. Gofer, D. Aurbach, J. Electrochem. Soc. 148 (2001) E155.
[23] N. Yamamoto, H. Hirasawa, H. Ishida, T. Tatsuma, N. Oyama, Bull. Chem. Soc. Jpn. 67 (1994) 1296.
[24] Y. Mo, Y. Gofer, E. Hwang, Z. Wang, D.A. Scherson, J. Electroanal. Chem. 409 (1996) 87.
[25] S. Koike, T. Fujieda, N. Wakabayashi, S. Higuchi, J. Power Sources 68 (1997) 480.
[26] D. Aurbach, M. Moshkovich, Y. Choen, A. Schechter, Langmuir 15 (1999) 2947.
[27] D. Aurbach, Y. Cohen, J. Electrochem. Soc. 144 (1997) 3355.
[28] D. Aurbach, Y. Cohen, J. Electrochem. Soc. 143 (1996) 3525.
[29] K. Morigaki, T. Fujii, A. Ohta, Denki Kagaku 66 (1998) 824.
[30] R. Mogi, M. Inaba, T. Abe, Z. Ogumi, J. Power Sources 97/98 (2001) 265.
[31] R. Mogi, M. Inaba, Y. Iriyama, T. Abe, Z. Ogumi, J. Electrochem. Soc., in press.
[32] D. Aurbach, J. Electrochem. Soc. 136 (1989) 906.
[33] D. Aurbach, M. Daroux, P. Faguy, E. Yeager, J. Electroanal. Chem. 297 (1991) 225.
[34] D. Aurbach, A. Zaban, J. Electrochem. Soc. 141 (1994) 1808.
[35] D.M. Kolb, M. Przasnyski, H. Gerischer, Electroanal. Chem. Interfacial Electrochem. 54 (1974) 25.
[36] D. Wagner, H. Gerischer, Electrochim. Acta 34 (1989) 1351.
[37] D. Pletcher, J.F. Rohan, A.G. Ritche, Electrochim. Acta 39 (1994) 1369.
[38] A. Zaban, D. Aurbach, J. Power Sources 54 (1995) 289.
[39] T. Osaka, T. Momma, Y. Matsumoto, Y. Uchida, J. Power Sources 68 (1997) 497.
[40] T. Fujieda, Y. Xia, S. Koike, M. Shikano, T. Sakai, J. Power Sources 83 (1999) 186.
[41] M. Klimmeck, K. Jüttner, Electrochim. Acta 27 (1982) 83.
[42] J. Sackmann, A. Bunk, R.T. Pötzschke, G. Staikov, W.J. Lorenz, Electrochim. Acta 43 (1998) 2863.
[43] Y. Geronov, F. Schwager, R.H. Muller, J. Electrochem. Soc. 129 (1982) 1422.
[44] M.W. Verbrugge, B.J. Koch, J. Electrochem. Soc. 141 (1994) 3053.
[45] A.V. Churikov, Electrochim. Acta 46 (2001) 2415.
[46] A. Zaban, E. Zinigrad, D. Aurbach, J. Phys. Chem. 100 (1996) 3089.
[47] S.G. Meibuhr, J. Electrochem. Soc. 118 (1971) 1320.
[48] N. Munichandraiah, L.G. Scanlon, R.A. Marsh, J. Power Sources 72 (1998) 203.